Volume 146
Number 9
7 May 2021
Pages 2737-3074

Analyst

rsc.li/analyst

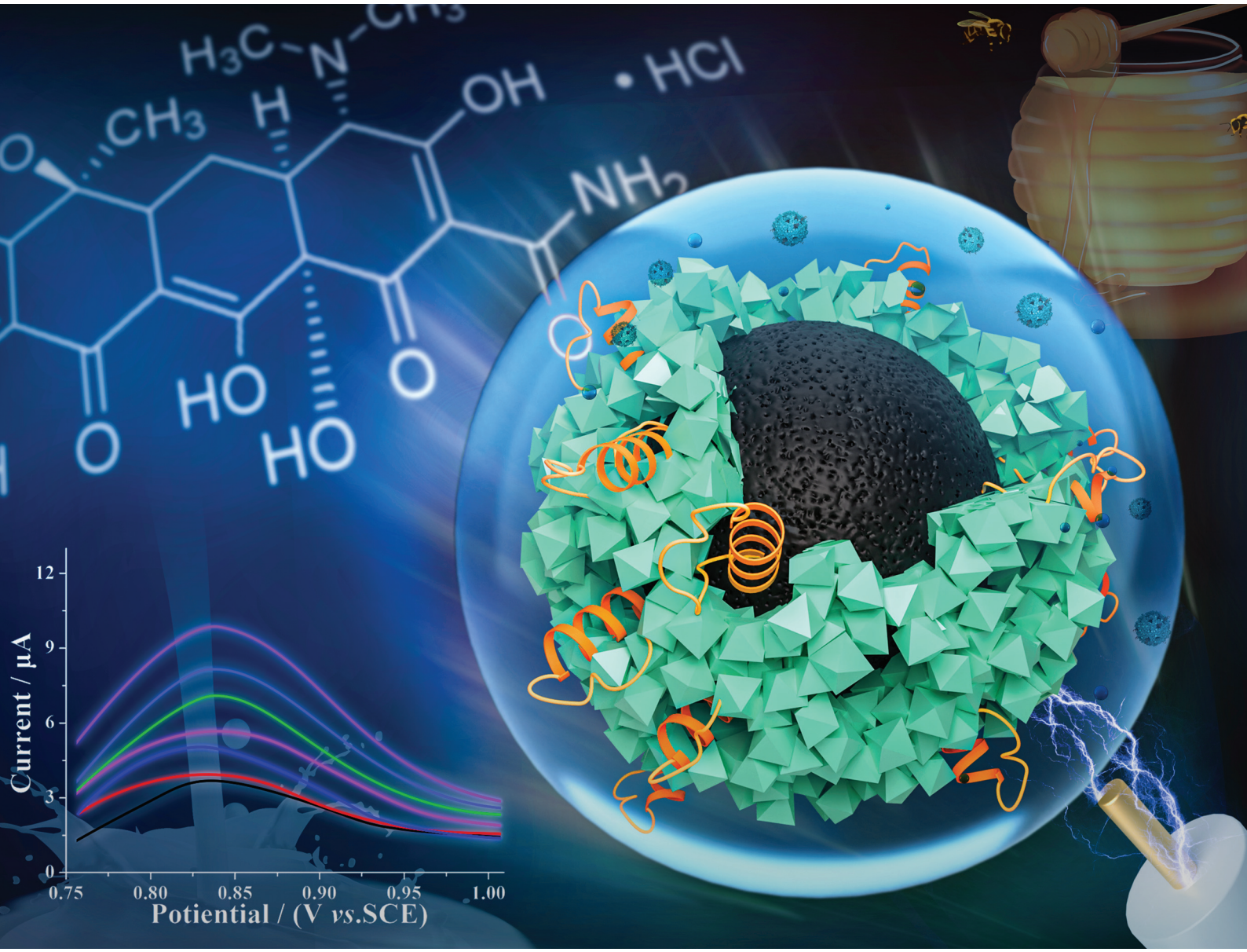

ISSN 0003-2654

ROYAL SOCIETY OF CHEMISTRY

PAPER

Jinhua Piao *et al.*

Fabrication and application of a novel electrochemical biosensor based on a mesoporous carbon sphere@UiO-66-NH_2/Lac complex enzyme for tetracycline detection

Analyst

ROYAL SOCIETY OF CHEMISTRY

PAPER

View Article Online
View Journal | View Issue

Cite this: *Analyst*, 2021, **146**, 2825

Fabrication and application of a novel electrochemical biosensor based on a mesoporous carbon sphere@UiO-66-NH_2/Lac complex enzyme for tetracycline detection†

Xiaomin Zhong,[a] Fang Wang,[b] Jinhua Piao *[a] and Yitao Chen[c]

The overuse of tetracycline results in a threat to human, poultry and livestock health. An enzymatic electrochemical biosensor is an ideal alternative method for accurate and rapid tetracycline detection, while the unstable and easily deactivated nature of the enzyme limits its development. To overcome these limitations, a highly sensitive enzymatic electrochemical biosensor for the determination of tetracycline is developed in this work based on a complex enzyme which was constructed using a mesoporous carbon sphere@UiO-66-NH_2 (MCS@UiO-66-NH_2) core–shell composite with embedded laccase (Lac). Compared to pure MCS and UiO-66-NH_2, the MCS@UiO-66-NH_2 core–shell composite has an advantageous mesoporous structure (pore diameter >8 nm), which is suitable for the immobilization of small laccase. The biosensor based on the complex enzyme exhibits a superior activity and enhanced stability as compared with that made using a pure enzyme because the mesoporous structure of the MCS@UiO-66-NH_2 composite can effectively protect the laccase against inactivation and denaturation. Besides, its high specific surface area and good conductivity are beneficial to enzyme immobilization and electron transfer in the modified electrode. The biosensor based on this complex enzyme exhibits a relatively low detection limit of 8.94×10^{-7} mol L^{-1} and a detection range of 1.0×10^{-6}–6.0×10^{-5} mol L^{-1} for tetracycline detection. Furthermore, the developed biosensor possesses good long-term stability, selectivity and reproducibility, indicating its potential application for tetracycline determination in actual food. This research work provides a prospective solution to resolve the stability and inactivation problems of enzymatic electrochemical biosensors in different application scenarios.

Received 21st December 2020,
Accepted 16th March 2021

DOI: 10.1039/d0an02430a

rsc.li/analyst

1. Introduction

Tetracycline (TC) has been widely used in agriculture, aquaculture, and animal husbandry because of its broad-spectrum antimicrobial activity against Gram-positive and Gram-negative bacteria and growth promotion properties.[1] However, the overuse of TC in stock farming results in certain serious risks including drug resistance of microbial strains and allergic reactions.[2–4] Therefore, the standard is relatively strict for TC residues in food products. For example, the National standard of China (GB31650-2019) regulated that the maximum oxytetracycline, chlortetracycline, tetracycline, single or in combination residues were 0.1 mg kg^{-1} for milk, 0.6 mg kg^{-1} for liver, 1.2 mg kg^{-1} for kidneys and 0.4 mg kg^{-1} for egg, respectively.[5] Thus, developing an accurate and sensitive method for the detection of TC is of great importance. Until now, various analytical methods have been developed for the detection and quantification of TC.[6,7] However, some inherent disadvantages, such as time-consumption, professional operation, complicated pre-treatment procedures and expensive equipment, have limited their wide applications to some extent.[6] Instead, electrochemical sensors came into the view as a competitive option for detecting antibiotics especially TC with the properties of quick response, accuracy, high sensitivity, inexpensiveness and simple pretreatment.[2,8–10] Compared to non-enzyme electrochemical sensors, enzymatic electrochemical biosensors are more widely investigated because of their high efficiency, good selectivity and high affinities toward corres-

[a]*School of Food Science and Engineering, South China University of Technology, Guangzhou 510641, Guangdong, PR China. E-mail: jhpiao@scut.edu.cn; Fax: +86-20-87113849; Tel: +86-20-87113849*
[b]*School of Environmental Engineering and Chemistry, Luoyang Institute of Science and Technology, Luoyang, 471023, PR China*
[c]*School of Life and Environmental Science, Guilin University of Electronic Technology, Guilin, 541004 Guangxi, PR China*
† Electronic supplementary information (ESI) available. See DOI: 10.1039/d0an02430a

ponding substrates.[11–13] However, there are only a few research studies to explore the possibilities of detecting TC by enzymatic electrochemical biosensors to our knowledge.

Laccase (Lac) (EC 1.10.3.2) is a copper-containing oxidase that can catalyze the oxidation of the phenolic and non-phenolic compounds, including some antibiotics and pesticides.[14] In recent years, a lot of projects have proved that laccase is useful in the degradation and removal of TC in water or the environment.[15,16] These studies indicate that laccase can catalyze the oxidation of TC using molecular oxygen as an electron acceptor under mediator presence.[17–19] Hence, we consider that it is possible to develop an enzymatic electrochemical biosensor based on laccase for tetracycline detection.

Generally, the performance of an enzymatic electrochemical biosensor is highly related to the catalytic activity and stability of the enzyme modified electrode.[14–16] There are some factors, such as extreme pH, heat, and long storage time, which can lead to the deactivation of enzymes when they are applied in various catalytic fields.[9,13,20] Meanwhile, the non-conducting protein of enzymes is prone to influence the electron transfer in the modified electrode. The poor long-term stability of the enzyme modified electrode under operating conditions also hinders its application. To improve these shortcomings, combining enzymes with a porous, high specific surface area and high conductivity material is an effective alternative method to enhance the enzymatic activities and improve its reusability, catalytic efficiency, and stability under drastic catalytic conditions.[21,22]

Metal organic frameworks (MOFs) which are constructed by the coordination of metal cations or clusters and organic ligands are an ideal support matrix for enzyme immobilization owing to their multifunctional properties involving a large surface area, ultra-high porosity and physical and chemical stability.[23–25] In particular, UiO-66, a zirconium-based MOF, consisting of a dodecadentate $Zr_6O_4(OH)_4$ cluster and a 1,4-benzene-dicarboxyl linker, has been widely applied in various fields, such as heterogeneous biomimetic catalysis,[26,27] food safety monitoring[24] and enzyme immobilization.[26] For example, Li *et al.* prepared a UiO-66-NH_2@PMAA (tethering polymethacrylic acid) composite to immobilize pectinase, which could adapt to a wider temperature and pH range and showed enhanced enzymatic activity and storage stability compared to free enzymes.[26] It indicates that UiO-66 is highly promising for laccase immobilization. Nevertheless, the poor conductivity of UiO-66 hinders its full potential of practical application. Combining it with good conductivity functional materials, such as carbon materials, metal nanoparticles and conducting polymers, can make up for the defects.[25,27–29] The mesoporous carbon sphere (MCS) possesses excellent conductivity, relatively high specific surface area and large total pore volumes.[30–33] Thus, it is expected that combining MCS with UiO-66 can develop a new enzyme supporting material which can improve the activity and stability of the enzyme modified electrode.

In this work, a novel enzymatic electrochemical biosensor based on a complex enzyme which consists of a mesoporous carbon sphere@UiO-66-NH_2 (MCS@UiO-66-NH_2) core–shell composite with embedded laccase was developed for tetracycline detection. In this biosensor, the as-prepared MCS@UiO-66-NH_2/Lac complex enzyme was used as a bio-recognition element, 2,2′-azino-bis(3-ethylbenzthiazoline-6-sulphonic acid) (ABTS) as a mediator and chitosan (CHIT) as a binder. The biosensor showed high catalytic activity and good stability compared with that made using pure laccase. Scheme 1 shows the construction process of the MCS@UiO-66-NH_2/Lac/ABTS/CHIT/GCE tetracycline biosensor. The advantageous mesoporous structure was formed during the preparation process of the MCS@UiO-66-NH_2 composite. Then, laccase was evenly embedded in the pores of the MCS@UiO-66-NH_2 core–shell composite matrix which can effectively protect the laccase against inactivation and denaturation. It is beneficial to improve the activity and stability of the complex enzyme-based biosensor. The reaction mechanism of the tetracycline oxidation on the biosensor is shown in Scheme S1.†[17] The reaction process on the complex enzyme-modified electrode surface may be followed the equations:[17]

$$\mathrm{Lac(Red)} + \mathrm{O_2} \rightarrow \mathrm{Lac(Ox)} + \mathrm{H_2O} \quad (1)$$

$$\mathrm{Lac(Ox)} + \mathrm{ABTS} \rightarrow \mathrm{Lac(Red)} + \mathrm{ABTS^{\bullet+}} \quad (2)$$

$$\mathrm{Lac(Ox)} + \mathrm{ABTS^{\bullet+}} \rightarrow \mathrm{Lac(Red)} + \mathrm{ABTS^{++}} \quad (3)$$

$$\mathrm{ABTS\text{-}e^-} \rightarrow \mathrm{ABTS^{\bullet+}} \quad (4)$$

$$\mathrm{ABTS^{\bullet+}\text{-}e^-} \rightarrow \mathrm{ABTS^{++}} \quad (5)$$

$$\mathrm{ABTS^{++}} + \mathrm{TC} \rightarrow \mathrm{ABTS^{\bullet+}} + \mathrm{TC(Ox)} \quad (6)$$

$$\mathrm{ABTS^{\bullet+}} + \mathrm{TC} \rightarrow \mathrm{ABTS} + \mathrm{TC(Ox)} \quad (7)$$

Tetracycline can be oxidized in the presence of laccase and ABTS. Firstly, laccase is oxidized with O_2 while ABTS is oxidized to $ABTS^{\bullet+}$ and $ABTS^{++}$ by oxidized laccase, and TC is oxidized during the reduction process of the $ABTS^{\bullet+}$ and $ABTS^{++}$.[17,32] The as-prepared enzymatic electrochemical bio-

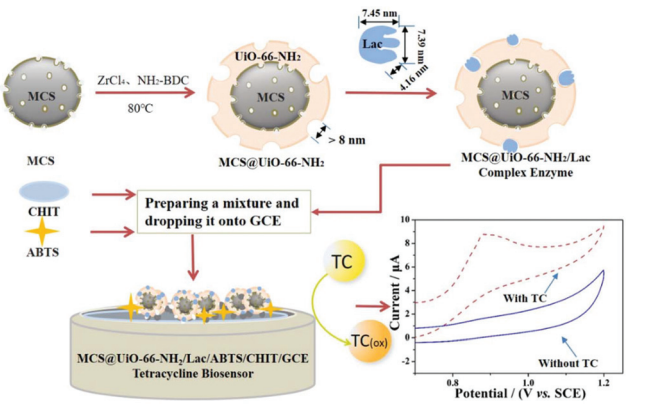

Scheme 1 Illustration of the synthesis process of the MCS@UiO-66-NH_2/Lac complex enzyme and construction of the MCS@UiO-66-NH_2/Lac/ABTS/CHIT/GCE tetracycline biosensor.

sensor can be applied to the detection of tetracycline in some TC-containing foods including water, milk, meat, honey and so on. The biosensor based on the complex enzyme provides a prospective solution to resolve the stability and inactivation problems of enzymatic electrochemical biosensors in different application scenarios.

2. Experimental

2.1 Materials and chemicals

Laccase that originated from *Trametes versicolor* (Lac, >5 U mg^{-1}) was purchased from Sigma-Aldrich (USA). Zirconium chloride ($ZrCl_4$, 98%), 1,4-benzenedicarboxylic acid (BDC, 98%), 2-amino benzene dicarboxylic acid (NH_2-BDC, 98%), benzoic acid (99.5%), *N*,*N*-dimethylformamide (DMF, 99.5%), tetraethylorthosilicate (TEOS, 98%), oxytetracycline (OTC, 98%), 2,2′-azino-bis(3-ethylbenzthiazoline-6-sulphonic acid) (ABTS, 98%), and tetracycline (TC, CP) were obtained from Shanghai Macklin Biochemical Co., Ltd (China). Chitosan (CHIT, deacetylation degree ≥95%) came from Cool Chemistry Technologies Co., Ltd (China). Streptomycin sulfate (SS, >590 U mg^{-1}) and neomycin sulfate (NS, MYM) were provided by MYM Biological Technology Co., Ltd (China). Milk came from Arla Foods (Denmark). Linden honey came from Fengzhichao Biological Engineering Co., Ltd (China). The 0.1 M sodium acetate–acetate buffer solution (HAc–NaAc) with different pH values was prepared by mixing 0.1 M HAc and 0.1 M NaAc solutions of different ratios. All chemicals and reagents were analytical grade reagents and used as received without any further purification.

2.2 Apparatus

The crystal structure of the prepared materials was characterized using an X-ray diffractometer (XRD, XD-3A, Shimadzu Corp., Japan) with Cu-Kα radiation at 40 kV in the range of 5–60° with a scanning speed of 12° min^{-1}. The morphology of the prepared materials was characterized by scanning electron microscopy (SEM, Zeiss Supra40, Germany). Chemical compositions were measured using an energy dispersive spectrometer (EDS). Fourier transform infrared spectroscopy (FTIR) was carried out using a Fourier Transform Infrared Spectrometer (Nicolet IS50, Thermo Fisher Scientific). The surface area and pore size distribution of the materials were measured by the nitrogen adsorption/desorption method at 77 K, recorded on a Micromeritics ASAP2460. The specific surface areas were calculated by the Brunauer–Emmett–Teller (BET) method, and the pore size distribution was calculated by the Barrett–Joyner–Halenda (BJH) model. The average size and size distribution of particles were analyzed using ImageJ software.[34]

Electrochemical measurements were carried out using a CHI 660E electrochemical analyzer (Shanghai Chenhua Instrument Co., Ltd, China) with a standard three-electrode cell. The as-prepared biosensors were used as the working electrode, a saturated calomel electrode (SCE) as the reference electrode, and a platinum sheet as the auxiliary electrode. The electrochemical performances were measured by cyclic voltammetry (CV), differential pulse voltammetry (DPV) and electrochemical impedance spectroscopy (EIS). EIS measurements were performed in the frequency range of 0.01 Hz to 1000 kHz. All the experiments were carried out at ambient temperature.

2.3 Preparation of the MCS@UiO-66-NH_2/Lac complex enzyme

The preparation of the MCS@UiO-66-NH_2/Lac complex enzyme followed a three-step procedure. Firstly, the MCS was prepared following the method reported previously with minor revision.[30,31] The detailed preparation process is presented in Scheme S2.† Next, the MCS@UiO-66-NH_2 core–shell composite was prepared. The preparation details are described in the ESI (Scheme S3†). After that, the synthesized MCS@UiO-66-NH_2 core–shell composites (20 mg) were dispersed in 20 mL of 5 mg mL^{-1} laccase solution (laccase in 0.1 M HAc–NaAc buffer solution, pH = 6) by stirring to form a uniform mixture, and then incubated at 4 °C for 12 h. Subsequently, the mixture was centrifuged and washed with 30 mL acetic buffer solution three times. After drying overnight at room temperature, the MCS@UiO-66-NH_2/Lac complex enzyme was finally obtained (Scheme 1).

2.4 Construction of the enzymatic electrochemical biosensor

First of all, the glassy carbon electrode (GCE, 3 mm diameter) was well polished using alumina powders (0.05 μm in diameter) on a polishing cloth and then rinsed with ethanol and distilled water in an ultrasonic bath for 5 min, respectively. The polished GCE was dried at room temperature. The as-prepared MCS@UiO-66-NH_2/Lac complex enzyme and ABTS were then homogeneously dispersed in the chitosan solution (1.0 wt%) to eventually form a mixed solution with a concentration of 40.0 mg mL^{-1} for the MCS@UiO-66-NH_2/Lac complex enzyme and 0.1 mM for ABTS. Finally, 5 μL of the mixture was dropped on the surface of the polished GCE. After drying at room temperature, the MCS@UiO-66-NH_2/Lac/ABTS/CHIT/GCE electrochemical biosensor was constructed. The process is represented in Scheme 1. For comparison, the modified electrodes ABTS/CHIT/GCE, UiO-66-NH_2/ABTS/CHIT/GCE, MCS@UiO-66-NH_2/ABTS/CHIT/GCE and Lac/ABTS/CHIT/GCE were also prepared using the same method. These biosensors were stored at 4 °C before use.

2.5 Application of the complex enzyme-based tetracycline biosensor in actual samples

Milk and honey samples were purchased from a local supermarket, Guangzhou, China. Briefly, 15 mL of milk and honey samples mixed with HAc–NaAc buffer solution (0.1 M, pH 5.5) at a volume ratio of 1 : 9, respectively. The MCS@UiO-66-NH_2/Lac/ABTS/CHIT/GCE biosensor was applied to detect the tetracycline content of the above mixtures employing the standard addition method.

3. Results and discussion

3.1 Structural and morphological characterization of the as-prepared materials

The as-prepared materials were characterized by several kinds of technologies to confirm their structure and morphology. The XRD patterns of the as-prepared materials are shown in Fig. 1. It can be seen that there are no obvious diffraction peaks originating from the MCS (a), indicating that the as-prepared mesoporous carbon sphere is an amorphous phase. The diffraction peaks of UiO-66 (c) and UiO-66-NH_2 (d) are similar to that of the simulated UiO-66 (b) reported previously.[25] It demonstrates that the UiO-66 and UiO-66-NH_2 materials were successfully prepared. It also can be found from Fig. 1 that the diffraction peak of the prepared MCS@UiO-66-NH_2 core–shell composite (e) is identical to that of UiO-66-NH_2 (d) and no new characteristic peaks appear. These results indicate that the microstructure of the UiO-66-NH_2 has not been damaged after compositing with MCS and no impurities are produced during the compositing process. It demonstrates that the MCS@UiO-66-NH_2 composite was synthesized successfully, which is also confirmed by the FTIR spectra (Fig. S1†) and further SEM results.

The nitrogen adsorption–desorption isotherms and pore size distribution plots of the as-prepared materials are depicted in Fig. 2. It can be found that the as-prepared MCS (curve a), UiO-66-NH_2 (curve b) and the MCS@UiO-66-NH_2 core–shell composite (curve c) all exhibit a type IV hysteresis loop, which is usually associated with the mesopores and capillary condensation.[31] For the UiO-66-NH_2 and the MCS@UiO-66-NH_2 core–shell composite, the nitrogen adsorption–desorption isotherms show a step at *ca.* 0.1 of P/P_0 according to the micropore filling process, indicating micropore structure existence in these two materials.[27] The two samples also show that the quantity adsorbed increases sharply after the relative pressure higher than 0.9. The reason may be that adsorbent condensation happens. The inset in Fig. 2 is the pore size distribution curves obtained by the BJH

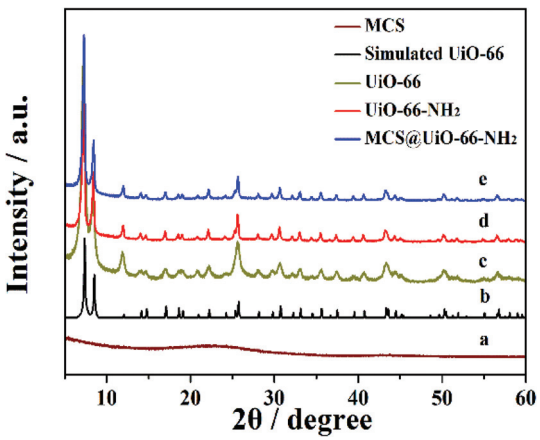

Fig. 1 XRD patterns of the as-prepared materials.

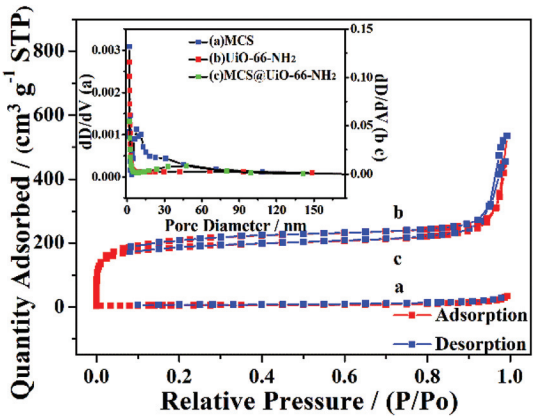

Fig. 2 The nitrogen adsorption–desorption isotherms: (a) MCS, (b) UiO-66-NH_2, and (c) MCS@UiO-66-NH_2 composite; the inset is the pore size distribution calculated by the BJH method of the three materials.

method. The pore size distribution of the pores exhibits a strong peak at about 7 nm for the MCS, and the MCS@UiO-66-NH_2 composite possesses a wider pore size distribution. It suggests that a lot of mesopores with different pore sizes are produced during the formation process of the MCS@UiO-66-NH_2 composite. The parameters of the as-prepared materials are calculated and listed in Table S1.† The MCS achieves the lowest specific surface area of 18.96 $m^2\ g^{-1}$ and pore volume of 0.05 $cm^3\ g^{-1}$. The UiO-66-NH_2 has the highest specific surface area of 773.37 $m^2\ g^{-1}$, and the pore volume is 0.45 $cm^3\ g^{-1}$. The specific surface areas of the MCS@UiO-66-NH_2 composites are examined to be 700.89 $m^2\ g^{-1}$, slightly below that of the UiO-66-NH_2. It may be caused by the existence of a low specific surface area of the MCS in the MCS@UiO-66-NH_2 composite. However, the MCS@UiO-66-NH_2 composite retains the highest pore volume of 0.59 $cm^3\ g^{-1}$. The average pore size is 7.04 nm for the MCS, 2.47 nm for UiO-66-NH_2 and 17.37 nm for the MCS@UiO-66-NH_2 composite, respectively. The relatively high surface area, pore diameter and pore volume of the MCS@UiO-66-NH_2 composite make it suitable for small laccase immobilization.

The morphologies of the prepared materials were characterized by SEM. As displayed in Fig. 3A, the morphologies of the MCS are clearly observed as regular spheres with a rough surface. The average size of the MCS is 2691.48 ± 491.02 nm (Fig. S2A and B†). Fig. 3B shows that the well-synthesized UiO-66-NH_2 particles possess rough cubic crystals and have a broad distribution range of particle size from 80–120 nm. From the image of Fig. 3C, it can be seen that the UiO-66-NH_2 nanoparticles are multilevel to surround the surface of the carbon sphere to form MCS@UiO-66-NH_2 core–shell composites. And the particle size of UiO-66-NH_2 in the composite decreases evidently as compared with that of UiO-66-NH_2 prepared independently. Many large opening pores are produced inside the accumulated UiO-66-NH_2 particles. The result can explain the reason for the increase of the average pore diameter and pore volume of the MCS@UiO-66-NH_2 composite

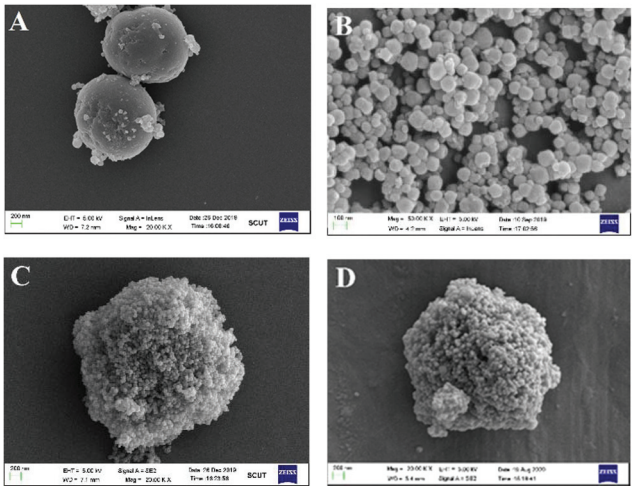

Fig. 3 SEM images of the as-prepared materials: (A) MCS, (B) UiO-66-NH_2, (C) MCS@UiO-66-NH_2 composite, and (D) MCS@UiO-66-NH_2/Lac complex enzyme. The scale bars: 200 nm for (A), (C) and (D), 100 nm for (B).

(Table S1†). The average size of the MCS@UiO-66-NH_2 composites is 3900.62 ± 482.86 nm (Fig. S2C and D†). The particles of the MCS and MCS@UiO-66-NH_2 composites are roughly monodisperse. After compositing with enzymes, the morphologies of the MCS@UiO-66-NH_2 composite have no significant change (Fig. 3D).

EDS analysis was performed for further confirming the micro-structure of the MCS@UiO-66-NH_2/Lac complex enzyme and the corresponding elemental mappings are shown in Fig. 4. The results prove the structure of the MCS@UiO-66-NH_2 composite and confirm the enzyme immobilization on it. Fig. 4A is the electron image of the as-prepared complex enzyme. Fig. 4B–D are the mapping images of different elements. It can be seen that the C (only from MCS) element (Fig. 4B), Zr (only from UiO-66-NH_2) element (Fig. 4C) and S (only from laccase) element (Fig. 4D) are obviously dense in the centre circular region, indicating that the MCS@UiO-66-NH_2 composite exists and the laccase is successfully immobilized on the MCS@UiO-66-NH_2 composite.

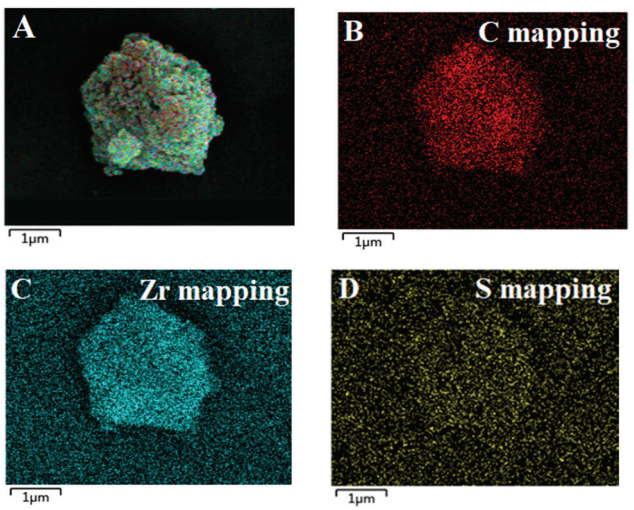

Fig. 4 EDS mapping results of the MCS@UiO-66-NH_2/Lac complex enzyme: (A) electron image, (B) C mapping, (C) Zr mapping and (D) S mapping.

The possible process was proposed to explain the formation of the MCS@UiO-66-NH_2/Lac complex enzyme. On the basis of the aforementioned, massive mesopores formed during the accumulation process of UiO-66-NH_2 on the MCS core, and the average pore size of the MCS@UiO-66-NH_2 composite is 17.37 nm (Table S1†). Therefore, the small laccase with a measured size of about 7.45 nm × 7.39 nm × 4.16 nm (ref. 33) can be embedded in the mesopores of the MCS@UiO-66-NH_2 composites by absorption. Then, the MCS@UiO-66-NH_2/Lac complex enzyme was successfully constructed. The laccase loading on the MCS@UiO-66-NH_2 composite reached a maximum value of 155.08 mg g^{-1} (Fig. S3†) at an initial laccase concentration of 5 mg mL^{-1}.

Zeta-potential has been used in enzyme immobilization to reveal the electrostatic interactions between an enzyme and its supporting material.[35] As shown in Fig. S4,† the zeta-potential of the prepared MCS@UiO-66-NH_2 composite is −1.91 ± 0.18 mV at the immobilization pH of 6.0. Besides, the isoelectric point (pI) of free laccase from *Trametes versicolor* is pH 2.8 and has a negative zeta-potential (about −26 mV) at pH 6.0.[36] It can be demonstrated that there is no electrostatic attraction between the laccase and supporting composites because the charges of the laccase (pI = 2.8) and MCS@UiO-66-NH_2 composite are both negative. Consequently, it is not the electrostatic attraction but only mesoporous adsorption that can favour the embedding of the enzyme at the immobilization pH of 6.0.

3.2. Electrochemical properties of the fabricated biosensor

Cyclic voltammetry is a common and effective method to investigate the electrochemical properties of modified electrodes. The CV curves of the as-prepared different biosensors were characterized in 0.1 M HAc–NaAc buffer solution (pH = 5.0) containing 5 mM $[Fe(CN)_6]^{3-/4-}$ and 0.1 M KCl at a scan rate of 100 mV s^{-1}. As a mediator, ABTS exists in all types of modified electrodes except the bare GCE. As shown in Fig. 5A, there is a pair of well-defined redox peaks for the CV curve of

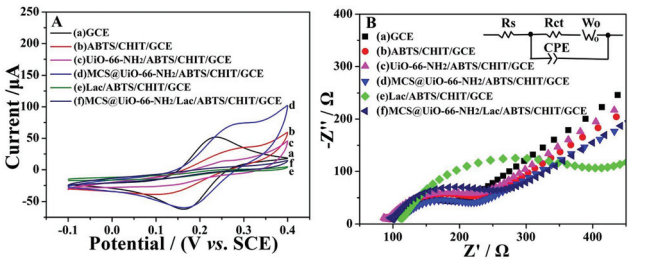

Fig. 5 Electrochemical properties of different modified electrodes: (A) CV curves and (B) Nyquist plots, the inset is the equivalent circuit model.

the bare GCE (curve a). After decorating with chitosan, UiO-66-NH_2 and laccase, respectively, the peak currents (curves b, c and e) all decrease obviously because of their poor conductivities. The peak current increases evidently for the MCS@UiO-66-NH_2 composite modified electrode (curve d) as compared with that of UiO-66-NH_2 modified electrodes (curves c). It indicates that the existence of MCS in the MCS@UiO-66-NH_2 composite avails the electron transfer in the modified electrode. As compared with the MCS@UiO-66-NH_2 modified electrode (curve d), the peak current of the MCS@UiO-66-NH_2/Lac complex enzyme modified electrode (curve f) decreases evidently, which is attributed to the blocking of electron transfer by enzyme protein. Meanwhile, the peak current of the MCS@UiO-66-NH_2/Lac/ABTS/CHIT/GCE modified electrode is higher than that of the Lac/ABTS/CHIT/GCE modified electrode (curve e), demonstrating that the complex enzyme containing the MCS@UiO-66-NH_2 composite can improve the response current signal of the enzyme electrode.

The EIS of the fabricated biosensors were measured to further illustrate the electrochemical properties of the fabricated biosensor. The Nyquist plots of the as-prepared different modified electrodes are given in Fig. 5B. The fitted results are shown in Table S2.† The semicircle diameter of the Nyquist curve equals electron transfer resistance (R_{ct}) for the $[Fe(CN)_6]^{3-/4-}$ redox probe, which controls the electron transfer kinetics of the modified electrode. R_s refers to solution ohmic resistance. As shown in Fig. 5B and Table S2,† the R_{ct} values of all types of electrodes except the MCS@UiO-66-NH_2/ABTS/CHIT/GCE (curve d) are larger than that of the GCE (curve a). The Lac/ABTS/CHIT/GCE (curve e) shows the largest R_{ct} value. The R_{ct} values are 107.0, 134.2, 143.2 and 286.8 Ω for the GCE (curve a), ABTS/CHIT/GCE (curve b), UiO-66-NH_2/ABTS/CHIT/GCE (curve c) and Lac/ABTS/CHIT/GCE (curve e) (Table S2†), respectively. The reason is that non-conductive chitosan, UiO-66-NH_2 and laccase influence the electron transfer in the modified electrode and result in the increase of R_{ct} values. The MCS@UiO-66-NH_2/ABTS/CHIT/GCE (curve d) exhibits the smallest Nyquist semicircle diameter (Fig. 5B) and the R_{ct} value is 104.4 Ω because the excellent conductivity of MCS is beneficial to electron transfer in the modified electrode. After compositing with laccase, the R_{ct} value increases to 158.8 Ω for the MCS@UiO-66-NH_2/Lac/ABTS/CHIT/GCE (curve f). The EIS results are in accordance with the results of CV (Fig. 5A). The results of CV and EIS all illustrate that the complex enzyme is helpful to improve the response signal of the modified electrode as compared with the pure enzyme.

3.3. Electrochemical behaviour of the complex enzyme-based biosensor toward TC

In order to determine the effects of the MCS@UiO-66-NH_2/Lac complex enzyme on the electrocatalytic activity and stability of the biosensors, the electrochemical behaviours of the as-prepared biosensors toward TC were evaluated using CV methods. Fig. 6 gives the CV curves for the Lac/ABTS/CHIT/GCE and the MCS@UiO-66-NH_2/Lac/ABTS/CHIT/GCE biosensors in the absence and presence of TC. It can be seen that there are no

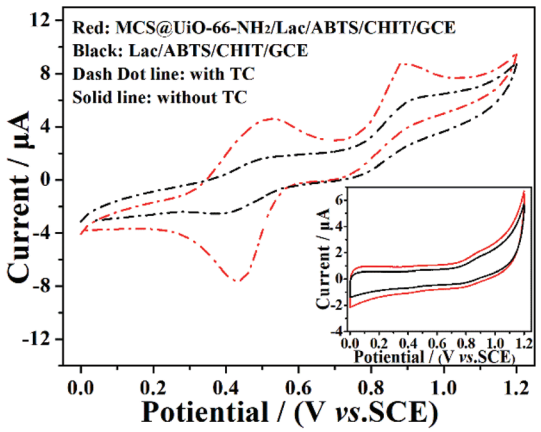

Fig. 6 CV curves of the as-prepared biosensors in the absence and presence of TC.

obvious current responses for both electrodes in the absence of TC (solid line). When 30 μM of TC was added, obvious current signals appear at about 0.51 V and 0.85 V *vs.* SCE (dash not line) for both the electrodes. Meanwhile, the response signal of the biosensor made using the MCS@UiO-66-NH_2/Lac complex enzyme increases evidently compared to that made using pure laccase. Based on the reaction mechanism of the tetracycline oxidation on the biosensor (eqn (1)–(7)), the anodic peaks at 0.51 V may come from a reversible one-electron oxidation of ABTS to $ABTS^{\bullet+}$ and the other (at about 0.85 V) derives from a second reversible one-electron oxidation of $ABTS^{\bullet+}$ to $ABTS^{++}$.[17] After the addition of TC, more ABTS molecules are present on the electrode surface. As a result, the currents of the anodic peak at about 0.51 V and 0.85 V all increase. These results certify that the biosensor based on laccase and ABTS can catalyze the oxidation of TC and the use of the MCS@UiO-66-NH_2/Lac complex enzyme to construct a biosensor can promote the response signal evidently due to the advantageous mesoporous structure, with high conductivity and large specific surface area of the MCS@UiO-66-NH_2 composite.

The stability of the Lac/ABTS/CHIT/GCE and the MCS@UiO-66-NH_2/Lac/ABTS/CHIT/GCE biosensors was also evaluated by the CV method. The response current decreases about 4.17% after ten cycles for the biosensor constructed by the MCS@UiO-66-NH_2/Lac complex enzyme (Fig. S5A†), and it decreases 28.81% for the biosensor made using pure laccase (Fig. S5B†). These results demonstrate that the complex enzyme possesses a superior catalytic activity and dramatically enhanced stability compared with the pure enzyme. The reason is that the mesoporous structure of the MCS@UiO-66-NH_2 core–shell composite can effectively protect the laccase against inactivation and denaturation.

Fig. S6† reveals the CV response of the MCS@UiO-66-NH_2/Lac/ABTS/CHIT/GCE biosensor which was measured in the 0.1 M HAc–NaAc buffer solution (pH 5.5) containing 30 μM TC at different scan rates from 25 to 200 mV s^{-1}. It shows that the current response increased gradually with the increase of the

scan rates (Fig. S6A†). The peak current of TC oxidation has a good linear relationship with the scan rate (R^2 = 0.9825) (Fig. S6B†). It suggests that the oxidation of TC on the MCS@UiO-66-NH_2/Lac/ABTS/CHIT/GCE biosensor is a surface controlled process.

3.4 Optimization of experimental parameters of the complex-enzyme-based biosensor

In order to improve the electrochemical sensing performance of the biosensor in the determination of TC, the experimental parameters were optimized by DPV in 0.1 M HAc–NaAc buffer solution containing 30 μM tetracycline at a scan rate of 100 mV s^{-1}. During the optimization process, all parameters were kept invariable except the parameter under study. The loading amount of the enzyme in the modified electrode can strongly influence its catalytic performance. Therefore, the effect of the concentration of the MCS@UiO-66-NH_2/Lac complex enzyme on the response current of the complex enzyme-based biosensor was firstly investigated. As shown in Fig. S7,† the catalytic current initially goes up with the MCS@UiO-66-NH_2/Lac complex enzyme concentration increase and shows the highest value at a concentration of 30 mg mL^{-1}. After that, the catalytic current decreases. Therefore, the concentration of the MCS@UiO-66-NH_2/Lac complex enzyme of 30 mg mL^{-1} was chosen to construct the biosensor in this work.

ABTS as a mediator may undergo the oxidation of TC with the use of different concentrations. The lack of ABTS in the TC biosensor based on laccase may hinder the oxidation of TC due to the lack of radical cation $ABTS^{\bullet+}$.[17] As shown in Fig. S8,† the response current increases with the ABTS concentration augment and the highest catalytic current value appears at a concentration of 0.10 mol L^{-1}. After 0.10 mol L^{-1}, the current value displays a platform indicating that more ABTS is unhelpful for current signal enhancement. Therefore, the ABTS concentration of 0.10 mol L^{-1} was used in further experiments.

The pH value can greatly influence the activity of the enzyme because it exhibits diverse electrostatic charge and hydrogen bond interactions in different pH.[37] TC is an amphiprotic compound with three acidic groups and its structure will change under alkaline conditions. It is a disadvantage for the adsorption on the surface of the electrode.[7] Therefore, the optimization of pH values was performed from 5.0 to 7.0 (Fig. S9†). It can be seen that the peak current is the highest at pH of 5.5. Hence, pH 5.5 was chosen to use in the following experiments.

3.5. Analytical performance of the complex enzyme-based biosensor

The linear range of the as-prepared MCS@UiO-66-NH_2/Lac/ABTS/CHIT/GCE biosensor for TC was evaluated by DPV measurement in the 0.1 M HAc–NaAc buffer solution under optimal conditions. Fig. 7 indicates that the response currents increase gradually with the augment of the TC concentration and there is a good linear relationship between the oxidation peak current and TC concentrations from 1.0×10^{-6} to 6.0×10^{-5} mol L^{-1} (inset in Fig. 7). The linear equation is expressed as: $I(\mu A) = 0.1017C\ (\mu M) + 2.8173$ with a correlation coefficient of R^2 = 0.9860, in which I and C are the response current and TC concentration, respectively. The limit of detection (LOD) was calculated by the IUPAC (International Union of Pure and Applied Chemistry) method to be 8.94×10^{-7} mol L^{-1}. Compared to the results of some previously reported electrochemical sensors (Table S3†), the MCS@UiO-66-NH_2/Lac/CHIT/GCE enzymatic electrochemical biosensor in our work possesses a relatively low limit of detection and a wide linear range.

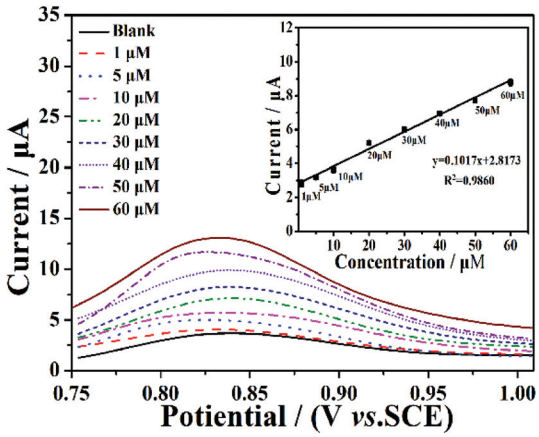

Fig. 7 Current responses of the MCS@UiO-66-NH_2/Lac/ABTS/CHIT/GCE biosensor for different concentrations of TC in 0.1 M HAc–NaAc buffer solution (pH 5.5); the inset is the linear relationship between the response current and TC concentrations.

3.6. Selectivity, reproducibility and stability of the complex enzyme-based biosensor

Selectivity is an important property for the enzymatic electrochemical biosensor, which determines whether the biosensor can be used in actual samples. The effects of interferents including OTC, SS and NS on the response current of the MCS@UiO-66-NH_2/Lac/ABTS/CHIT/GCE biosensor were analyzed by the DPV method. Comparison of response currents between four antibiotics and HAc–NaAc buffer solution has been explored. From Fig. 8, it can be found that the current caused by 30 μM tetracycline is obviously higher than those from 30 μM other antibiotics. Besides, there is no significant difference between the currents from the three interferents and buffer solution. Compared to the response current of buffer solution, the currents only increase 2.81% for NS, 2.90% for SS and 4.33% for OTC. The result shows that the biosensor based on the complex enzyme possesses satisfactory selectivity for TC.

The reproducibility of the biosensor was also determined under the same conditions using five batches of the complex enzyme-based tetracycline biosensor. There is a low relative standard deviation (RSD) value of 1.60%, which confirms a

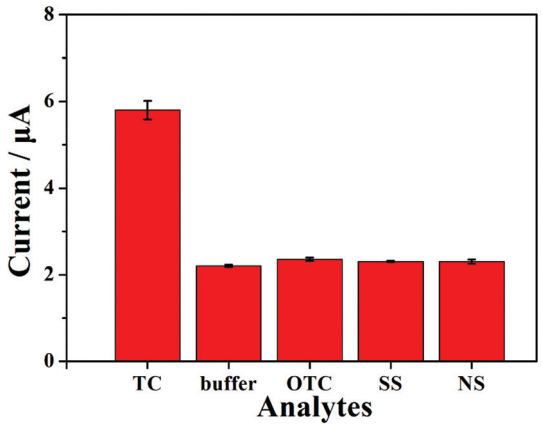

Fig. 8 The effect of interferents on the response current of the MCS@UiO-66-NH_2/Lac/ABTS/CHIT/GCE biosensor.

good reproducibility for the biosensor. The long-term stability of the MCS@UiO-66-NH_2/Lac/ABTS/CHIT/GCE biosensor was evaluated by the DPV responses toward TC in 0.1 M HAc–NaAc buffer solution (pH 5.5) containing 30 μM TC. The data were recorded every three days. The response currents decrease 2.54%, 6.46% and 11.81% after storage of the biosensor at 4 °C for three, six and nine days, respectively. It suggests that the as-prepared biosensor is well preserved and possesses good stability. This is mainly due to adequate protection by the mesopores of the MCS@UiO-66-NH_2 composite in the designed complex enzyme. It can be concluded that the MCS@UiO-66-NH_2/Lac/ABTS/CHIT/GCE biosensor has a good long-term stability and reproducibility.

The MCS@UiO-66-NH_2 composite plays a crucial role in protecting the enzyme and increasing its longevity in two ways. On the one hand, the MCS@UiO-66-NH_2 composite can be considered as a shell to protect enzymes dispersing in the mesopores from harsh conditions such as heat, pH, organic solvents and so on.[38] On the other hand, the aggregate of enzymes can be avoided and the conformation change of enzymes can be restricted due to the limited pore space, which can lead to the enhancement of structural rigidity of the immobilized enzyme.[21] For example, Pang *et al.* synthesized a bimodal micro-mesoporous Zr-metal organic framework to immobilize laccase, which showed an enhanced stability and a wider utilization range.[39] In a word, the mesoporous structure of MCS@UiO-66-NH_2 composite can effectively protect the laccase against inactivation and denaturation and increases its longevity.

3.7. Application of the complex enzyme-based biosensor in actual food samples

In order to further evaluate the performance of the MCS@UiO-66-NH_2/Lac/ABTS/CHIT/GCE biosensor in practical application, milk and honey samples were purchased from a local supermarket. The actual sample analysis of milk and honey was performed by the standard addition method. Three different concentrations (10, 20, 50 μM) of TC standard solution were spiked into the known-amount of 10% diluted milk and honey samples and then measured with amperometric measurement. The obtained results are shown in Table 1. Not all the contents of TC both in milk and honey are found. The recoveries range from 94.3% to 103.8% for the two samples. And RSD (n = 3) is lower than 6.0% and 11.7% for milk and honey samples, respectively. Thus, the prepared biosensor is a promising and reliable tool for the sensitive and rapid determination of TC in actual food samples.

Table 1 Recovery for the determination of TC in milk and honey

Samples	Added (μM)	Detected (μM)	Recovery (%)	RSD (%)
Milk	10	10.38	103.81	5.1
	20	18.86	94.32	6.0
	50	47.83	95.65	5.5
Honey	10	9.49	94.88	11.7
	20	19.12	95.60	5.4
	50	48.83	97.66	3.3

4. Conclusions

In summary, a sensitive and selective enzyme electrochemical biosensor was constructed based on the MCS@UiO-66-NH_2/Lac complex enzyme for the detection of TC. This work improved the activity and stability of laccase by embedding it onto the MCS@UiO-66-NH_2 core–shell composite to prepare a complex enzyme. The superior conductivity of the MCS@UiO-66-NH_2 composite can enhance the electron transfer in the modified electrode, and the mesopore structure of the MCS@UiO-66-NH_2 core–shell composite is beneficial to immobilize the laccase which can effectively protect the laccase against inactivation and denaturation. Under the optimum conditions, the biosensor displays a relatively low detection limit, wide linear range, and good selectivity, stability and reproducibility. It has great potential in application and can be produced in a relatively easy process. The biosensor can be applied for the detection of TC in various actual foods.

Conflicts of interest

There are no conflicts to declare.

Acknowledgements

This work has received funding from the National Natural Science Foundation of China (nos. 21975079 and 21968031) and the Natural Science Foundation of Guangdong Province of China (no. 2017A030313045).

Notes and references

1 Y. Wang, L. Yao, G. Ning, Y. Wu, S. Wu, S. Mao and G. Q. Liu, *Biosens. Bioelectron.*, 2019, **143**, 111613.
2 B. Ashe, L. N. Nguyen, F. I. Hai, D.-J. Lee, J. P. van de Merwe, F. D. L. Leusch, W. E. Price and L. D. Nghiem, *Int. Biodeterior. Biodegrad.*, 2016, **113**, 169–176.
3 C. B. Van Houten, A. Cohen, D. Engelhard, J. P. Hays, R. Karlsson, E. Moore, D. Fernández, R. Kreisberg, L. V. Collins, W. De Waal, K. M. De Winter-De Groot, T. F. W. Wolfs, P. Meijers, B. Luijk, J. J. Oosterheert, R. Heijligenberg, S. U. C. Sankatsing, A. W. J. Bossink, A. Stubbs, M. Stein, S. Reisfeld, A. Klein, R. Rachmilevitch, J. Ashkar, I. Braverman, V. Kartun, I. Chistyakov, E. Bamberger, I. Srugo, M. Odeh, E. Schiff, Y. Dotan, O. Boico, R. Navon, T. Friedman, L. Etshtein, M. Paz, T. M. Gottlieb, E. Pri-Or, G. Kronenfeld, E. Simon, K. Oved, E. Eden and L. J. Bont, *Eur. J. Clin. Microbiol. Infect. Dis.*, 2019, **38**, 505–514.
4 L. Chen, S. Yang, Y. Huang, B. Zhang, F. Kang, D. Ding and T. Cai, *J. Hazard. Mater.*, 2019, **371**, 566–575.
5 National food safety standard-Maximum residue limits for veterinary drugs in foods, the National Standard of the People's Republic of China, GB31650-2019, 2019, 28.
6 Z. R. Dizavandi, A. Aliakbar and M. Sheykhan, *Electrochim. Acta*, 2017, **227**, 345–356.
7 S. Kurbanoglu, S. A. Ozkan and A. Merkoçi, *Biosens. Bioelectron.*, 2017, **89**, 886–898.
8 H. Guo, Y. Su, Y. Shen, Y. Long and W. Li, *J. Colloid Interface Sci.*, 2019, **536**, 646–654.
9 M. Besharati, J. Hamedi, S. Hosseinkhani and R. Saber, *Bioelectrochemistry*, 2019, **128**, 66–73.
10 A. Benvidi, S. Yazdanparast, M. Rezaeinasab, M. D. Tezerjani and S. Abbasi, *J. Electroanal. Chem.*, 2018, **808**, 311–320.
11 J. Yoon, S. N. Lee, M. K. Shin, H.-W. Kim, H. K. Choi, T. Lee and J.-W. Choi, *Biosens. Bioelectron.*, 2019, **140**, 111343.
12 C. Feng, J. Guo, G. Li, B. Ye and L. Zou, *Sens. Actuators, B*, 2021, **326**, 128972.
13 A. Mahadevan and S. Fernando, *Biosens. Bioelectron.*, 2017, **92**, 417–424.
14 J. Yang, Y. Lin, X. Yang, T. B. Ng, X. Ye and J. Lin, *J. Hazard. Mater.*, 2017, **322**, 525–531.
15 X. Wen, Z. Zeng, C. Du, D. Huang, G. Zeng, R. Xiao, C. Lai, P. Xu, C. Zhang, J. Wan, L. Hu, L. Yin, C. Zhou and R. Deng, *Chemosphere*, 2019, **222**, 865–871.
16 M. de Cazes, M.-P. Belleville, M. Mougel, H. Kellner and J. Sanchez-Marcano, *J. Membr. Sci.*, 2015, **476**, 384–393.
17 M. Fabbrini, C. Galli and P. Gentili, *J. Mol. Catal. B: Enzym.*, 2002, **16**, 231–240.
18 K. Sun, Q. Huang and S. Li, *J. Hazard. Mater.*, 2017, **331**, 182–188.
19 J. Schwarz, M.-O. Aust and S. Thiele-Bruhn, *Chemosphere*, 2010, **81**, 1469–1476.
20 A. Wong, M. Scontri, E. M. Materon, M. R. V. Lanza and M. D. P. T. Sotomayor, *J. Electroanal. Chem.*, 2015, **757**, 250–257.
21 Y. Hu, L. Dai, D. Liu, W. Du and Y. Wang, *Renewable Sustainable Energy Rev.*, 2018, **91**, 793–801.
22 Z. Hu, R. Xu, S. Yu, J. Li and Z. Yang, *Analyst*, 2020, **145**, 7864–7869.
23 F. Wang, T. Feng, X. J. Jin, Y. L. Zhou, Y. J. Xu, Y. H. Gao, H. S. Li and J. F. Lei, *Chem. Eng. J.*, 2020, DOI: 10.1016/j.cej.2020.127583.
24 P.-L. Wang, L.-H. Xie, E. A. Joseph, J.-R. Li, X.-O. Su and H.-C. Zhou, *Chem. Rev.*, 2019, **119**, 10638–10690.
25 J. H. Cavka, S. Jakobsen, U. Olsbye, N. Guillou, C. Lamberti, S. Bordiga and K. P. Lillerud, *J. Am. Chem. Soc.*, 2008, **130**, 13850–13851.
26 Y. Li, J. Liu, K. Zhang, L. Lei and Z. Lei, *Ind. Eng. Chem. Res.*, 2018, **57**, 559–567.
27 M. J. Katz, Z. J. Brown, Y. J. Colón, P. W. Siu, K. A. Scheidt, R. Q. Snurr, J. T. Hupp and O. K. Farha, *Chem. Commun.*, 2013, **49**, 9449.
28 Y. Xue, B. Tian, M. Wang, T. Zhai, R. Li and L. Tan, *Colloids Surf., A*, 2020, **591**, 124549.
29 L. Valenzano, B. Civalleri, S. Chavan, S. Bordiga, M. H. Nilsen, S. Jakobsen, K. P. Lillerud and C. Lamberti, *Chem. Mater.*, 2011, **23**, 1700–1718.
30 H. Xie, J. Chong, Y. Tian and X. Wang, *J. Porous Mater.*, 2019, **26**, 185–191.
31 X. Xiao, B. Han, G. Chen, L. Wang and Y. Wang, *Sci. Rep.*, 2017, **7**, 40167.
32 T. Suda, T. Hata, S. Kawai, H. Okamura and T. Nishida, *Bioresour. Technol.*, 2012, **103**, 498–501.
33 T. Skálová, J. Dohnálek, L. H. Østergaard, P. R. Østergaard, P. Kolenko, J. Dušková, A. Štěpánková and J. Hašek, *J. Mol. Biol.*, 2009, **385**, 1165–1178.
34 L. Haddick, W. Zhang, S. Reinhard, K. Möller, H. Engelke, E. Wagner and T. Bein, *Pharmaceutics*, 2020, **12**, 505.
35 N. Schultz, G. Metreveli, M. Franzreb, F. H. Frimmel and C. Syldatk, *Colloids Surf., B*, 2008, **66**, 39–44.
36 A. Kołodziejczak-Radzimska, A. Budna, F. Ciesielczyk, D. Moszyński and T. Jesionowski, *Process Biochem.*, 2020, **95**, 71–80.
37 L. Wu, X. Lu, K. Niu, Dhanjai and J. Chen, *Biosens. Bioelectron.*, 2020, **165**, 112407.
38 S.-L. Cao, D.-M. Yue, X.-H. Li, T. J. Smith, N. Li, M.-H. Zong, H. Wu, Y.-Z. Ma and W.-Y. Lou, *ACS Sustainable Chem. Eng.*, 2016, **4**, 3586–3595.
39 S. Pang, Y. Wu, X. Zhang, B. Li, J. Ouyang and M. Ding, *Process Biochem.*, 2016, **51**, 229–239.